Effects of Microwave and Conventional Heat-Treatment on Additively Manufactured Stainless Steel

Thesis

Submitted in fulfilment of the requirements of

BITS F421T Thesis

By

Karthik Subramaniam

2019A4TS0602P

Under the supervision of

Dr Radha Raman Mishra, Assistant Professor of BITS Pilani

Dr Gururaj Telasang, Scientist of ARCI Hyderabad

BIRLA INSTITUTE OF TECHNOLOGY AND SCIENCE PILANI, PILANI CAMPUS

DECEMBER 2022

Acknowledgements

I would like to thank my supervisor Prof. Radha Raman Mishra for guiding me through the course of this Thesis. I would also like to thank Prof. Srikanta Routroy and the Mechanical Department of BITS Pilani for the opportunity to work on this thesis. I would also like to thank Mr Lachana Dora for his assistance through the course of this project.

I would also like to thank Dr Tata N Rao, Dr Ravi Bathe and Dr Gururaj Telasang of ARCI Hyderabad for the opportunity to work in their advanced facility and providing the required materials.

Certificate

This is to certify that the thesis entitled, “*Effects of Microwave and Conventional Heat-Treatment on Additively Manufactured Stainless Steel*” and submitted by Karthik Subramaniam, ID No. 2019A4TS0602P in partial fulfilment of the requirements of BITS F421T Thesis embodies the work done by him under my supervision.

Supervisor
Dr Radha Raman Mishra
Assistant Professor
Mechanical Engineering Department
BITS Pilani, Pilani Campus
Date:

Thesis Title: Effects of Microwave and Conventional Heat-treatment on Additively Manufactured Stainless Steel

Supervisor: Dr Radha Raman Mishra

Semester: First Session: 2022-2023

Name: Karthik Subramaniam ID: 2019A4TS0602P

Abstract

Additive manufacturing is layer-by layer manufacturing of components based on 3D design data. The process of selective laser melting has many parameters to it that can be altered to give a more desirable build component. The effect of post-manufacture heat-treatment on the microstructure and mechanical properties of Additively Manufactured Austenitic Stainless Steel has been investigated and reported. The heat-treatment was performed by both methods at 500°C for varying soaking times. The microwave heated samples showed fewer cracks as well as more redistribution of ferrite phases, implying more recrystallization than conventional heating.

Table of Contents

List of Figures

List of Tables

Chapter 1

Introduction

1.1 Introduction to Additive Manufacturing

Additive Manufacturing (AM) refers to a process by which digital 3D design data is used to build up a component in layers by depositing material. It has gone by other names at different time periods such as 3D printing, Rapid Prototyping, layered manufacturing, etc. AM manufactures by taking digital 3D design data and depositing material in the same fashion layer by layer. Broadly, melting of powders, Direct deposition, or extrusion are the 3 methods by which this is achieved. FDM (Fused Deposition Modelling) deposits fused material layer by layer through extrusion process. Binder Jetting (BJ) uses a liquid bonding agent to bond material powders layer by layer. All additive Manufacturing processes have some common parameters, such as scan speed and layer thickness. In general, a faster scan speed will reduce the manufacturing time but is also allows for more mistakes. Similarly, higher layer thickness means a faster build, but a core coarse design as any inclines or curves will appear as made of stepped layers [2].

Additive manufacturing has become more popular in recent years due it its short lead times and total design freedom. The ability to customize each build in its own way is very attractive. A lot of material is also saved compared to conventional subtractive manufacturing and so it preferred for expensive or rare materials.

1.2 Selective Laser Melting as an AM process-

The focus of this report is a specific PBF (Powder Bed Fusion) process - SLM (Selective Laser Melting). The material deposition in this process is done by melting of material powder using a high-power laser. The scanned layers are allowed to cool before a new layer of powder is deposited on top. This is done by a recoater spreading powder evenly on the build platform. The build platform is free to move in the z-axis and the laser scans in the x-y plane. The process is done in an inert atmosphere of Nitrogen or Argon to prevent combustion. There are many process parameters to keep in mind when working with SLM.

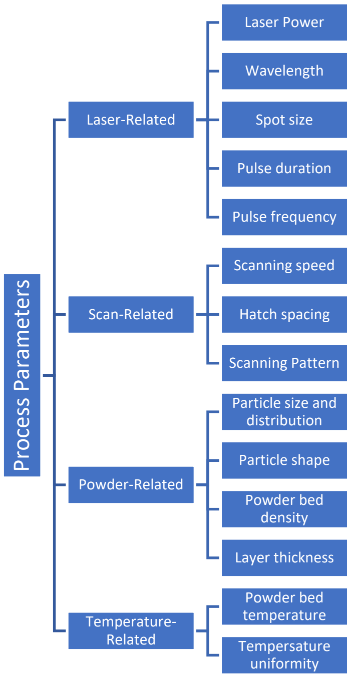

Figure 1- Process parameters for Selective Laser Melting

SLM is a process primarily used for metal alloy powders, including stainless steel, Nickel based superalloys, Titanium alloys, Aluminium alloys, etc. A laser (or pair of lasers) scans a powder bed, melting a layer of the metal powder before a new layer of metal powders is deposited over the previous layer. The build platform moves downwards so the build can move upwards layer by layer. After the build is done, any leftover powder can be collected and recycled for a new build.

Layer scanning is divided into bulk scanning, down-skin and up-skin. Down skin layers are specially scanned to penetrate deeper into the powder bed

Some common errors and defects found in SLM built parts are

Spheroidisation- If the metal powder is not evenly spread, large number of isolated metal balls will be formed.

Porosity- SLM is prone to porosity which reduces the mechanical properties of the built parts.

Incomplete Fusion Holes- When metal powders are not fully melted, it can lead to poor bonding or unmelted solitary powders.

Cracks- With the high cooling rate of 10^8 K/s (rapid melting ang cooling), a high temperature gradient causes thermal stress and thus can lead to cracks.

1.3 Aim and Motivation

The aim of this project is to study Additive Manufacturing of Stainless Steel and compare microwave and conventional heating of the additively manufactured steel.

In contrast to conventional heating, microwaves interact with materials in a different way. The ‘cold’ microwaves cause the material itself to generate heat, and so the heating can be rapid, uniform, and selective. When implemented properly, time and energy can be saved.

The hypothesis of this study is that the microwaves will interact with the Additively Manufactured stainless steel differently than conventional heating will. The presumption going into the study is that the steel will obtain a similar microstructural change at a lower energy cost. Consequently, the null hypothesis is that microwave heating will have no different effects on the microstructure and mechanical properties of the SLM-built steel.

Chapter 2

Literature Survey

2.1 SLM-built SS316L

SS 316 is a common alloy of Stainless Steel. It is composed of primarily Iron, with 16-18% chromium, 10-14% Nickel, 2-3% Molybdenum as well as trace amounts of Manganese, Carbon, Sulphur, Silicon and Phosphorous [1]. The stainless-steel alloy 316 is an austenitic steel that has properties of good ductility, a low deformation rate during cooling, and easy manipulation (bending or stretching). Stainless steels are widely used in the marine, biomedical, and aerospace industries owing to the combination of desirable mechanical properties, relatively low cost, and excellent corrosion resistance [4].

Traditionally, stainless steel parts have been manufactured using casting, forging, forming, squeeze casting or other conventional means. However, complex parts cannot directly be formed this way and there is also a limit to the mechanical properties achievable this way. Laser Additive manufacturing has gained a lot of interest for manufacturing stainless steel components for aerospace, automotive and biomedical applications.

The AM process resembles traditional welding in that both use a localized heat source to melt material to be reformed. This results in refined grain structure, directional grain-growth and oxidation in the fusion zone. How they differ is that in welding, the 2 joint parts are microstructurally homogenous with the weld being alien. In AM however, the microstructure is constant throughout the body. While errors are bound to be present, AM errors are getting better documented along with new techniques to mitigate those issues as the amount of research in this field steadily increases.

2.2 Mechanical Properties of SLM-built SS316L

Stainless Steel 316 is one of the few additively manufactured alloys that show both high strength and elongation despite porosity [5]. SLM fabricated stainless steel parts show significantly higher mechanical properties when compared to cast parts of same composition and dimensions. Results show the additively manufactured parts to be significantly harder with higher yield and tensile strengths. As a trade-off, when additively manufactured, SS becomes more brittle [6]. This phenomenon is observed as the strength-ductility trade off. As the strength increases, to preserve the energy under the graph, the extent of plastic deformation decreases. There is no noticeable distance in the fatigue life of additively manufactured SS316 [7].

Since we know that the motion of dislocations governs plastic deformations. By controlling the microstructures evolved, it is possible to control the mechanical properties of the build parts. The microstructures evolved as a result of SLM are different from other and conventional methods due to the rapid cooling. The cooling rate of the fused metal is 10^3- 10^8 K/s [8]. Given that SLM is a process that involves rapid solidification and cooling, it is not clear to what extent the solute redistribution can be supressed and whether a solute trapping effect can be achieved during this process.

AM parts tend to have many surface defects despite its high hardness. Grinding is a very common post processing treatment for Metal Additive Manufacturing. Surface defects commonly seen are roughness, unmelted powders, voids, and cracks due to residual stresses. The rapid cooling also causes residual thermal stresses in the manufactured parts. These surface defects can be fixed by laser polishing, chemical polishing, abrasive polishing, mechanical polishing, or a hybrid of the above methods [9].

2.3 Effects of build parameters on build quality

As seen in Figure 1, there are many parameters to SLM. Changing any one of the parameters will lead to changes in the build quality, finish, density, and a host of other metrics. This study focuses on the scan speed, hatch distance, and the laser power. The scan speed is how fast the laser pointer travels over the powder bed. The hatch distance is the distance between 2 consecutive scan paths and the laser power is the amount of energy transferred by the laser per unit time.

Scanning pattern in SLM, particularly the Materialise Magics slicing software, is as shown in figure 2. There are 3 zones- the outer border, the infill, and the hatch at the interior. The parameters mentioned above will affect only the hatch and not the other two zones. Each scanned track is a melt pool. This melt pool is the smallest unit of SLM. Multiple melt pools put together create a layer and multiple layers create a build [10].

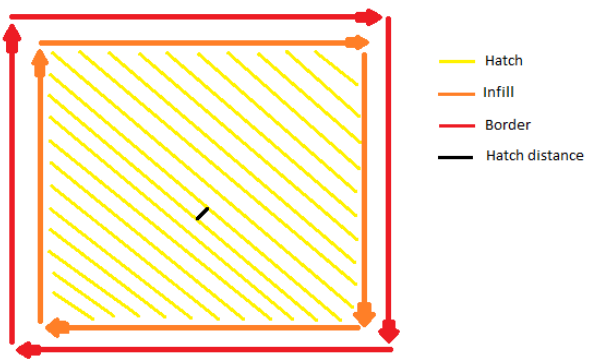

Figure 2- Scan paths in SLM

Increasing the scan speed will reduce the build time, but also leads to higher chances of incomplete fusion holes. However, a very slow scan speed can lead to melt pools that are too large and adversely affect the finish and bulk properties of the build. Increasing the hatch distance too much will lead to unmelted areas between scanned locations, but a very small hatch distance will lead to continuous melting and remelting of the powder. This will affect the microstructure and crystallization of the metal. If the laser power is too little, the melt pool won't be deep enough to penetrate the lower layers and inter-layer bonding will be weak, However, a very high laser power will again lead to the problems associated with a large melt pool. The ideal parameters for SLM are chosen taking all factors into consideration and their interaction with each other [11-12].

2.4 Effect of Heat Treatment

Heat treatment refers to the bulk heating of an additively manufactured part. It is a post processing technique that is used to change the properties of a built piece. Due to the rapid cooling and shear motion of the recoater, there are residual stresses in the built parts. Heat treatment is meant to take care of such residual stresses as well ask to adjust the microstructure to resemble more closely that of its conventionally manufactured counterparts. It is to be noted that annealing does not affect the XRD analysis of the material, implying that the crystal structure of the alloys does not change (microstructure and hardening).

As built microstructures display fan-shaped melt pool boundaries as a result of the high cooling rate. This often leads to very fine and irregular grains. High number of low angle grain boundaries allows for lots of scope for the boundaries to slip and form defects, potentially weakening the structure. Consequently, the extremely high grain boundary angle in the other direction is the reason for the high mechanical strength observed in as built stainless steel structures [12].

The columnar grains lead to strong mechanical properties in z direction (build-direction) but weak in the x-y plane. Heat treatment can reduce the severity of this anisotropy. Recrystallization can make the grains coarser, increasing the strength in the x-y plane while retaining much of the strength in the z-direction [14-17]. It has been seen that the strength and hardness of as built samples is the highest, and the more that the sample is heated, the strength and hardness falls and the ductility increases.

Temperature (°C)	Soaking time (mins)	Hardness (HV)	UTS (MPa)	Failure strain
400	60	290	760	15%
800	60	300	600	16%
950	30	220	610	16%
950	60	180	610	16%
950	120	170	630	17%
1100	30	160	580	16%
1100	60	160	560	20%

Table 1- Properties of SLM-manufactures SS316L after Heat Treatment [14-17]

2.5 Microwave heating of metals

Microwaves are electromagnetic radiations of wavelength between 1mm and 1m. They are an important constituent in many modern-day technologies such as medical treatments, networks and communications, food treatments, etc.

In contrast to conventional furnaces, materials in a microwave furnace interact with the ‘cold’ microwaves. As the material itself generates heat, the heating can be rapid, uniform and selective. When implemented properly, this allows microwave heating to reduce wasteful heating, save energy and hasten production. Microwave processing of powdered metals has been in the mainstream since 1999, when Dr Roy and his team sintered metal powders successfully to full density for the first time. Since then, many different sintering processes of copper, stainless steel, alumina powders, concrete, etc. have been done using microwaves for heating [26]. Most material powders can be heated in the microwave magnetic (H) field while only a few can be heated in the electric (E) field [18].

The interaction between the electric and magnetic fields that constitute microwaves, and the material often results in dielectric and magnetic losses. This is how microwaves heat materials. The dielectric losses mentioned before having been analysed and studied can be attributed to the redistribution of charges or polarization under the influence of an alternating external electric field. The nature of the dielectric polarization could be electronic, ionic, interfacial, or dipolar [19].

The needed particle size must be less than or equal to the metal's depth of penetration at the applied microwave frequency in order for metals to couple with microwaves directly. It is conceivable for the skin depth to exceed the particle size for small metal particles with a size of less than 3 microns at some point during the heating process. Additionally, charge accumulation at the particle ends may have an impact on the induced currents, changing the scattering patterns. The space between particles enables microwaves to penetrate further, and irregularly formed particles may affect the current flux or direction. Therefore, they reported that the microwave power penetration depth is significantly greater than the skin depth in a nonmagnetic metal powder and is estimated to be as much as 1 to 3 cm deep, depending on various factors such as particle size, bulk density, conductivity, oxide coating, etc [20-21].

Chapter 3

Materials and Methods

3.1 Materials and powder used

For this experiment, SS316L powders purchased from Oerlikon were used. The diameters of the particles have a distribution as shown in Figure 3. The mean diameter reported by Oerlikon is 45 microns, however the mean was found at 32 microns. These measurements were taken after sieving the powder using a sieve of pore size 90 micron. The size distribution was measured using a mastersizer 2000 built like Sciroco. Table 2 shows the chemical composition of the alloy used.

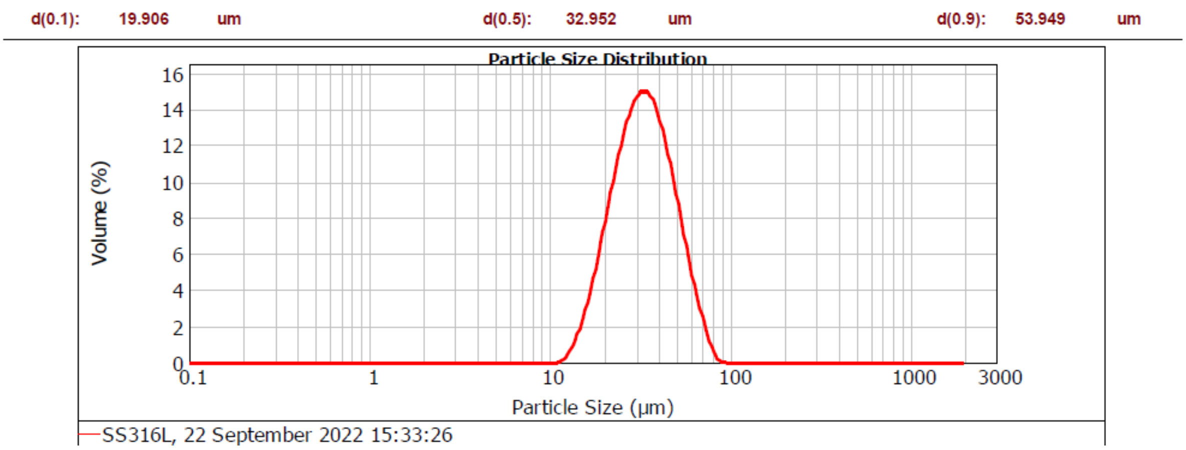

Figure 3- Particle size distribution of SS316L powder used.

Element	Fe	Cr	Mo	Ni	C	Other
Weight Percentage	Balance	18	12	2	<0.03	<1

Table 2- **Element composition of Alloy powder used.**

A total of 4 kilograms of powder was used, sieving in between each use. After every build, an average of 30g of oversized powder was collected. This powder would become oversized due to the sputtering and clumping phenomena. If oversize powder is allowed to pass through the tank, it will halt the build as it won't be able to pass through the powder reloader system. It will also cause scratches on the shaft which overtime will wear out the shaft.

3.2 Initial Experiments

The machine used for all experiments is a SLM solutions SLM280HL machine as shown in Figure 4. It is fitted with a maximum laser power of 400W, a spot size of 80µm and a wavelength of 1065nm. The parts were built on a preheated bed at 150°C and in a Nitrogen atmosphere.

Figure 4a- SLM Solutions SLM280HL Machine

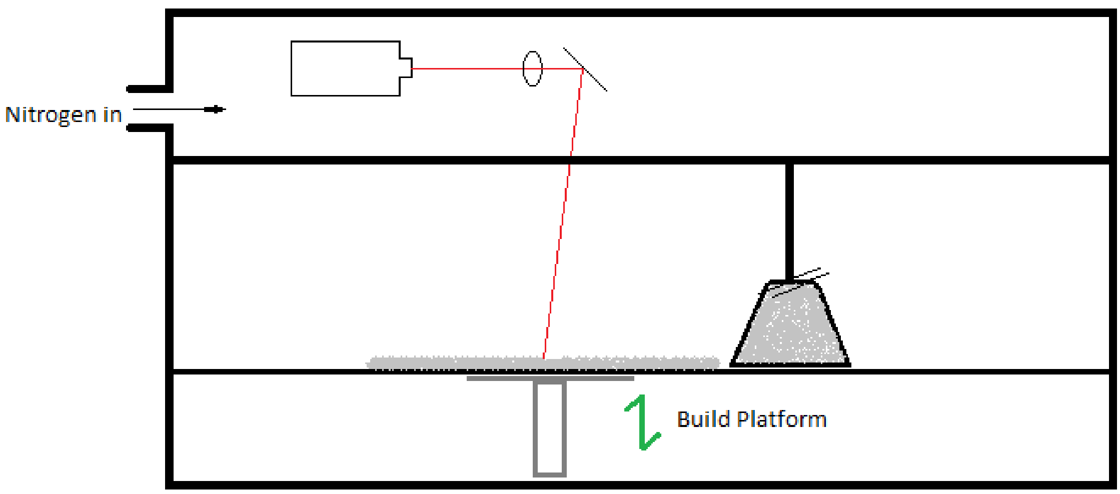

Figure 4b- Schematic drawing of SLM Process

To decide the build parameters, an initial experiment was performed to calibrate the machine. 9 test sample cuboids of 7mm x 5mm x 5mm were built with varying laser power, scan speed and hatch distances, as seen in Figure 5. The layer thickness had been decided at 50 micron. All parameters were varied in the hatch and the samples were built without an infill. The final build parameters were decided based on Archimedes density, hardness, and images of the built samples. Each cuboid was cut in half using an abrasive cutting machine. One half was used to test density and the other half was mounted in a thermoset polymer to be polished. These polished mounts were used for hardness testing and imaging using an optical microscope. The surface roughness was measured using a Mitutoyo SJ-410 portable surface roughness tester. All Figures 6 show apparatus used for testing.

Based on the data collected as seen in Table 3, __ was decided as the best parameters for the experiments. The build parameters were as follows- Layer thickness of 50 micron, Hatch distance of 0.11mm, laser power of 275W, and a scan speed of 700mm/s. The archimedes density is 7.64g/cm^3, as-build hardness 230HV. The as-built surface roughness is 6.08 micron and the surface roughness after sand blasting is 3.47 micron.

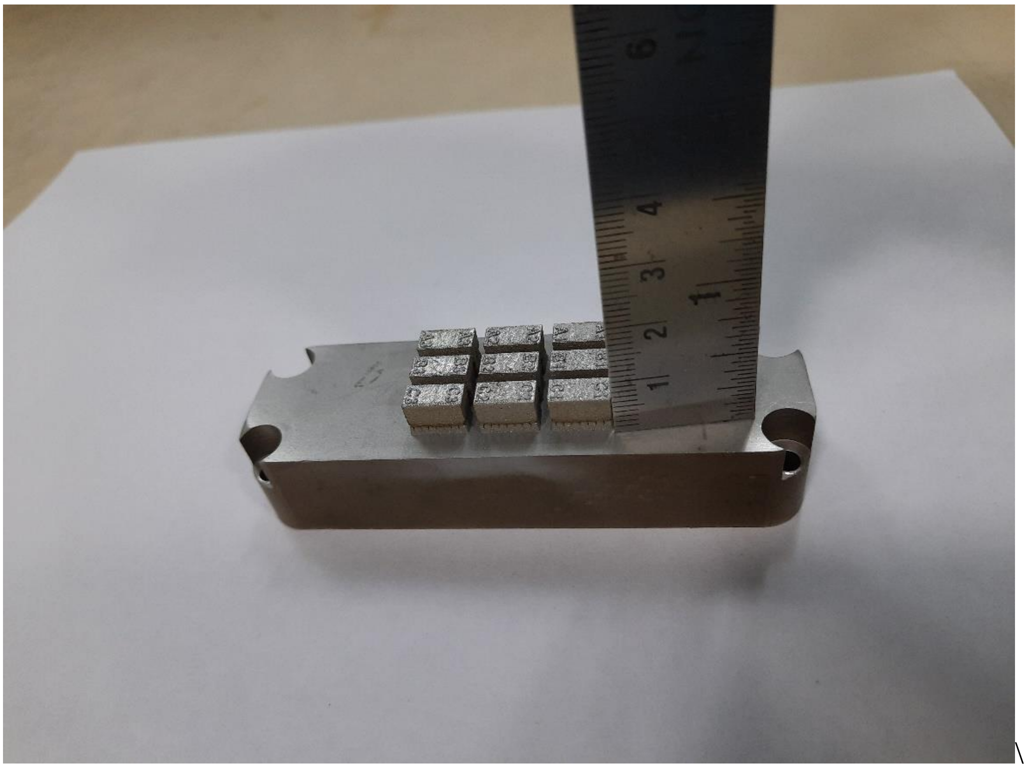

\

Figure 5- Initial experiment test cuboids, each built with different bulk parameters with label on top.

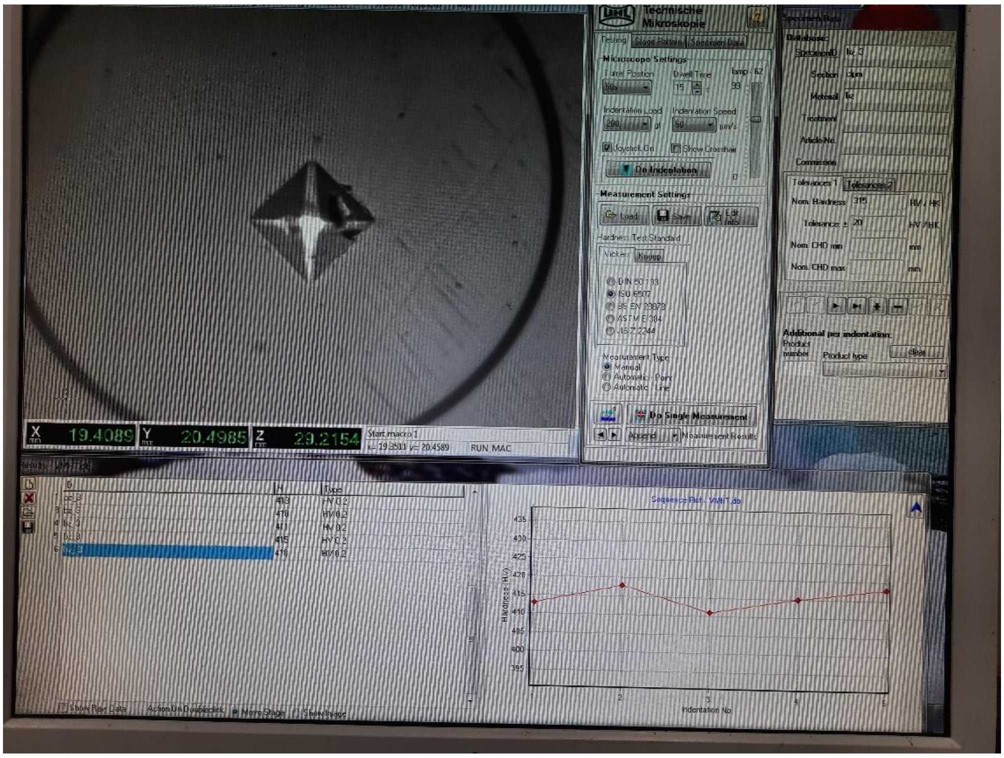

Figure 6(a)- Hardness test user interface.

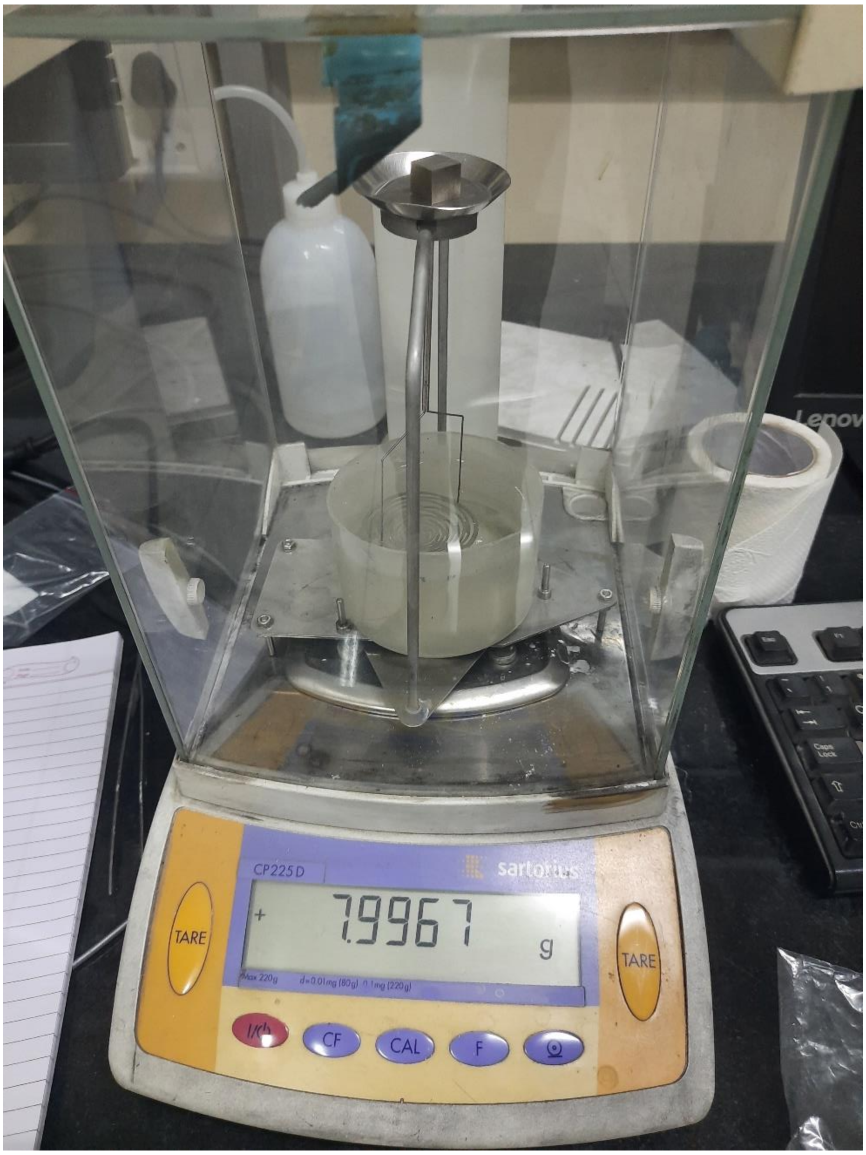

Figure 6(b)- Archimedes density test apparatus.

Sample Name	Scan Speed (mm/s)	Laser Power (W)	Hatch Distance (mm)	Density (g/cm^3)	Hardness (HV)
A1	300	900	0.1	7.42	210
A2	275	700	0.11	7.72	224
A3	250	700	0.12	7.64	230
B1	300	1000	0.1	7.70	204
B2	300	800	0.11	7.73	215
B3	275	700	0.12	7.76	228
C1	300	1000	0.09	7.76	220
C2	300	800	0.1	7.82	220
C3	300	700	0.11	8.57	248

Table 3- Initial experiment data to determine optimal build parameters.

3.3 Building samples

Each test coupon was built as a solid rod with diameter 9.5mm and length 57mm. Figure 7(a) shows the CAD model of the test coupon and Figure 7(b) shows the horizontally built test coupons and Figure 7(c) shows the vertically built samples. A total of 29 test coupons were built. Fifteen test coupons were built horizontally, split into three builds of six, six, and three and fourteen test coupons were built vertically in a single build.

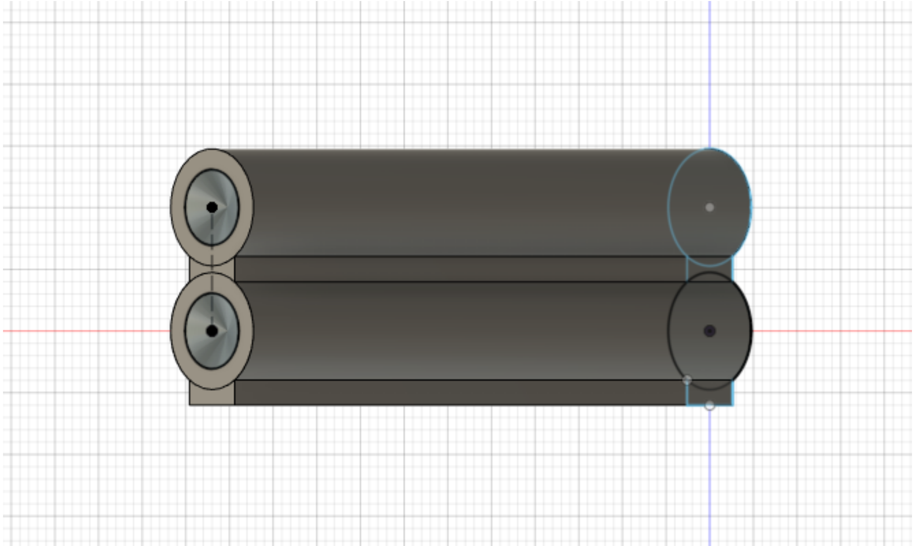

Figure 7(a)- CAD Model of tensile test coupon rods

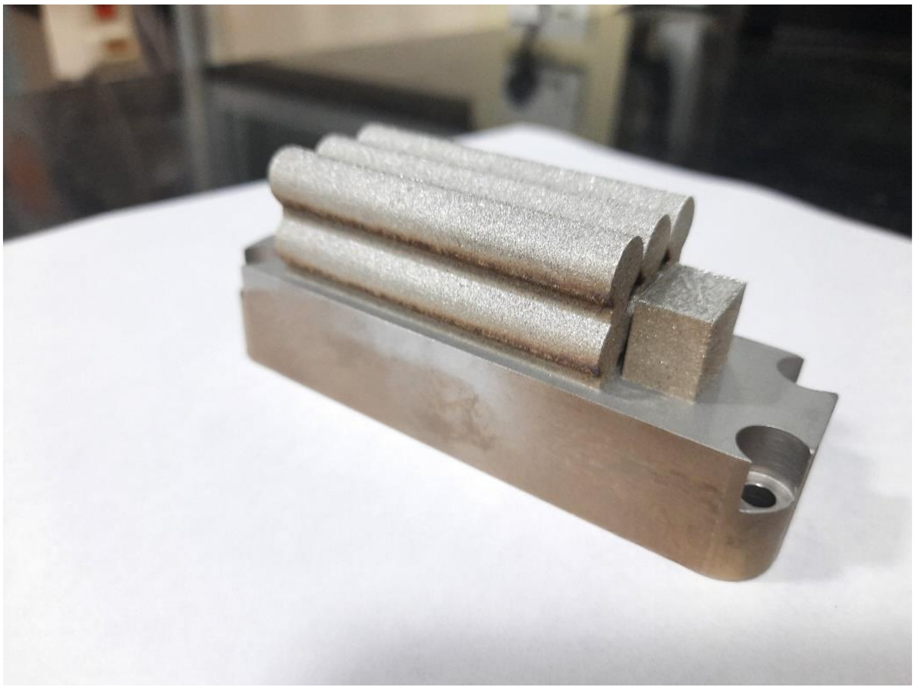

Figure 7(b)- Horizontally built tensile test coupons, along with a 7mm x 10mm x 15mm

Figure 7(c)- Vertically built tensile test coupons

The platform was heated to 150°C and the chamber was flooded with Nitrogen. The oxygen content by weight was maintained at less than 0.5% to avoid combustion. The minimum scan time (amount of time it takes to scan one layer from powder recoating to powder recoating) was a very dynamic setting. The crystallization time of the scanned surface would always change depending on the scanned surface area. depth achieved and, heat stored in the build. For the horizontal builds, the minimum scan time varied between 30s to 60s depending on which section of the build was being built. For the vertical build, the minimum scan time remained fairly constant at around 24s. When not handled properly, the recoater passing over fused metal will lead to large pores as the fused metal will stick to the recoating surface. Each horizontal build took a total of 9 hours for six test coupons and 4 hours for three test coupons. The verticle build took a total of 16 hours to complete. The samples are removed from the stainless-steel substrate using the ultima 2FA wire EDM machine.

Figure 8- All built test coupons, cut individually and sand blasted

3.4 Heating cycle and process

Looking at the data from Table 1, it was decided to try two heating cycles in the microwave furnace and one in the conventional furnace. The microwave furnace used is a VB Ceramic Consultants microwave furnace. It is built with 4 magnetrons for multi-directional heating. The conventional furnace used is a Harrier enterprises single zone split furnace. These can be seen in Figures 9 and 10.

Figure 9(a)- test coupon in the heating space of the microwave furnace.

Figure 9(b)- VBCC microwave furnace.

Figure 10- Harrier technologies conventional furnace.

The soaking temperature was set at 500°C. The two microwave heating cycles had a soaking time of 30 minutes and 60 minutes respectively. The conventional furnace heating cycle had a soaking time of 60 minutes. The heating rate was set at 5°C per minute and the conventional heating was done in a Nitrogen atmosphere.

3.4 Processing samples

After heating the samples, a portion of each was cut and polished for observing under SEM and Hardness test. The samples were cut using an abrasive cutting machine and then polished by hand on emery paper. The emery paper grades used were 80, 150, 220, 400, 600, 800, 1000, 1200, 1500, 2000, 2500, and 3000 in that order. After hand polishing, they were also semi-automatically polished on a cloth plate using a 6 micron diamond paste abrasive in an oil-based suspension.

Figure 11(a)- Hand polishing on emery paper

Figure 11(b)- Semi-automatic cloth polishing using diamond paste

Chapter 4

Results

The initial experiment was designed to test the machine's calibration and decide which parameters were best for the powder being used. Table 4 shows the density and porosity of all 9 of the test samples made and Figure 12 shows the hardness variation. Based on the data, sample A3 was chosen as ideal because it was a goof compromise of density and hardness. The maximum hardness samples were omitted because of low machinability. The low-density samples were omitted due to high porosity.

Sample Name	Density (g/cm^3)	Porosity percentage (%)
A1	7.42	6.00
A2	7.72	2.25
A3	7.64	3.30
B1	7.70	2.47
B2	7.73	2.16
B3	7.76	1.73
C1	7.76	1.75
C2	7.82	0.96
C3	8.57	4.11

Table 4- Density and porosity of test coupons

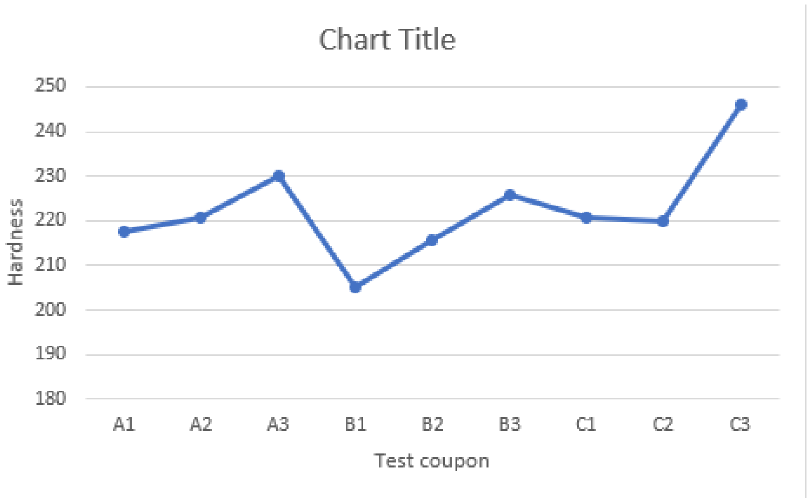

Figure 12- Hardness variation with test coupons

The polished samples were observed under Field Emission-Scanning Electron Microscope (FE-SEM, abbreviated to SEM for convenience). The SEM was manufactured by FEI, the Field Electron and Ion Company. SEM images were taken, and the following observations were made.

The samples when heated with microwaves for 60 minutes showed more redistribution of the Ferrite phase, whereas the conventionally heated samples showed the ferrite phase in a columnar structure. It was highly directional in the conventionally heated samples when compared to the fairly uniform and redistributed phases found in the microwave heated samples. These can be seen in Figures 13 and 14. In these figures, The ferrite phases are marked with red and the cracks are marked with yellow. All mentions of microwave heated samples are for the sample heated for 60 minutes at soaking temperature.

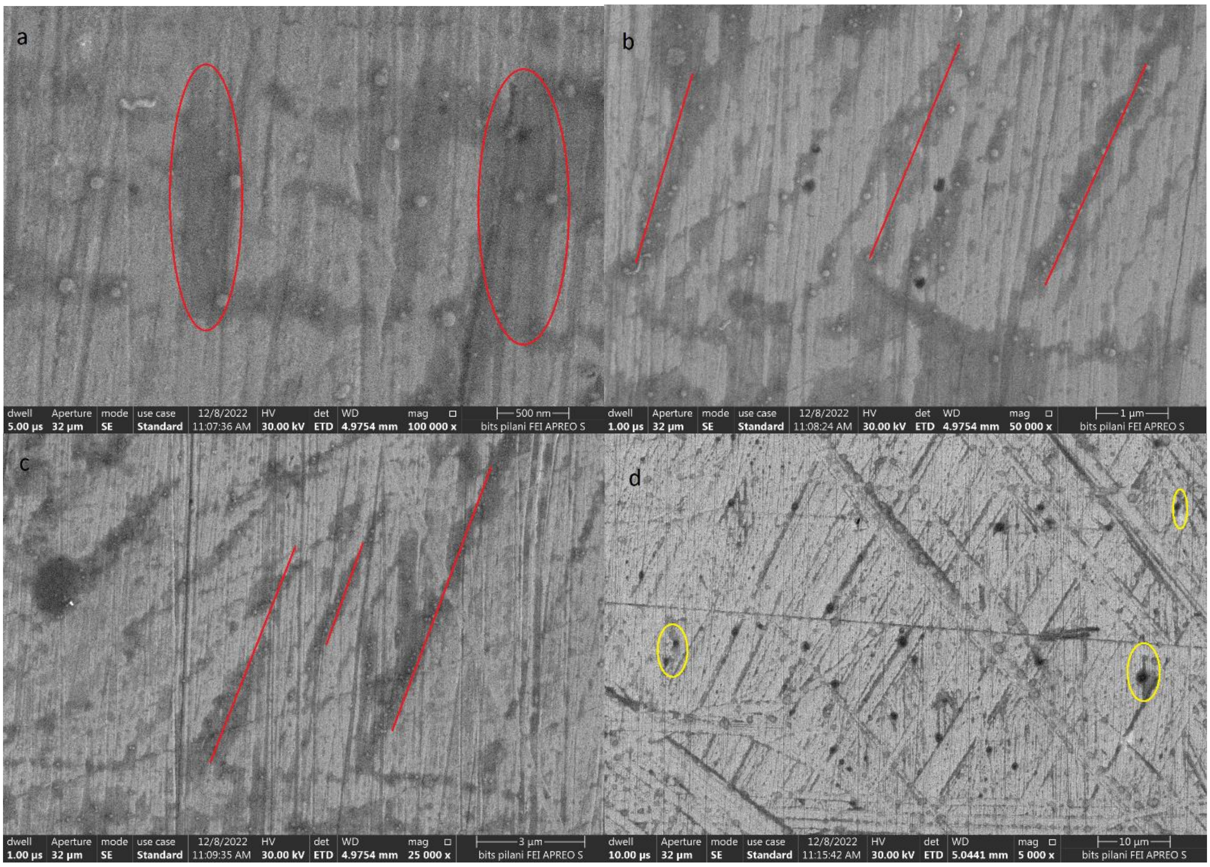

Figure 13- SEM images of conventionally heated sample. Magnifications are 100,000x, 50,000x, 25,000x, and 10,000x respectively

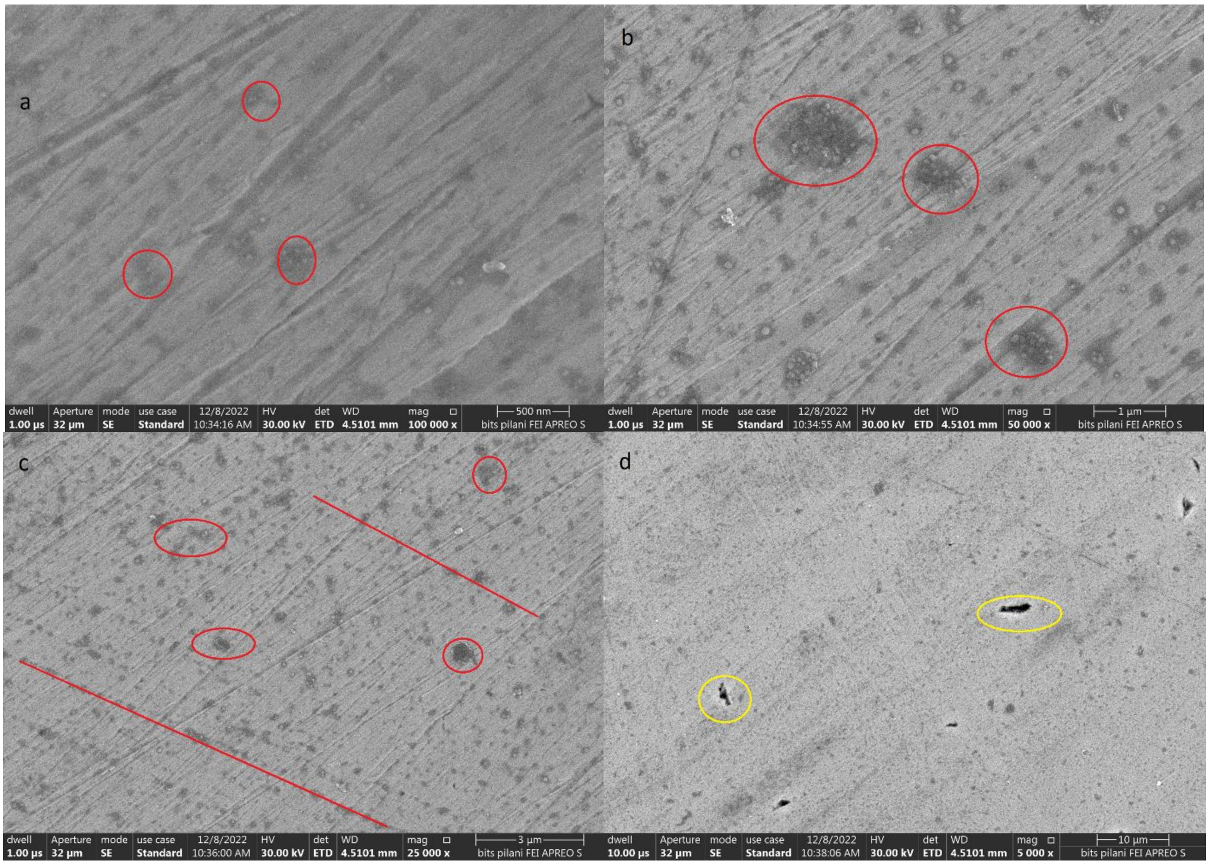

Figure 14- SEM images of conventionally heated sample. Magnifications are 100,000x, 50,000x, 25,000x, and 10,000x respectively

Figure 14c shows that the columnar structure is not entirely gone after microwave heating, but the phase is much more redistributed in the microwave heated sample than the conventionally heated sample.

This is likely due to microwave's bulk heating property. As the material directly interacts with microwaves and generated heat, the more ferrite phase clusters together. As seen is Figures 15 and 16, the heat maps of element distribution of both samples do not differ much, so the structures seen in Figures 13 and 14 are just phase redistributions.

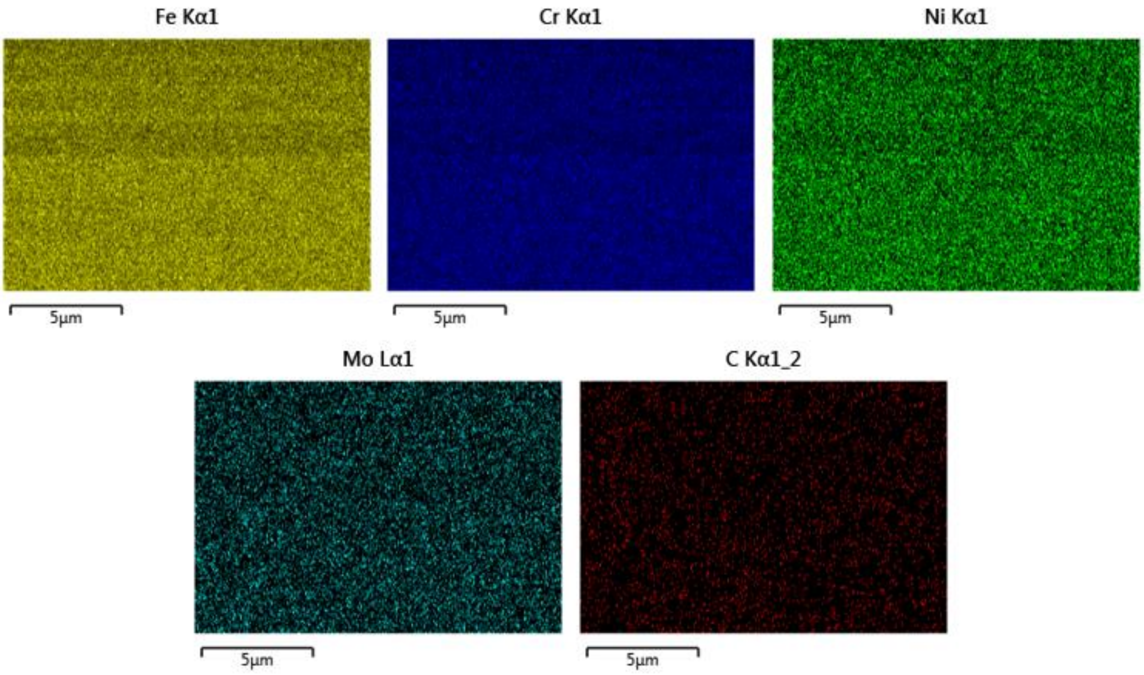

Figure 15- EDS heat distribution of elements in the microwave heated sample at 25,000x magnification.

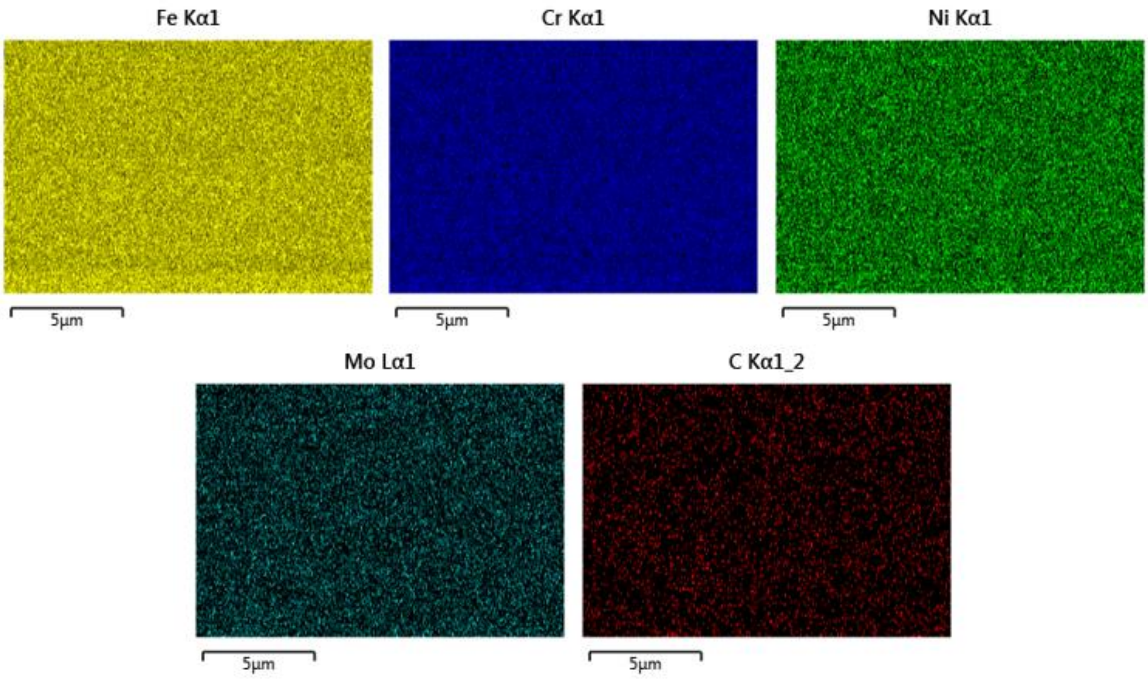

Figure 15- EDS heat distribution of elements in the microwave heated sample at 25,000x magnification.

The sample that was heated for 30 minutes showed extensive scratches and so no data could be reliably extracted.

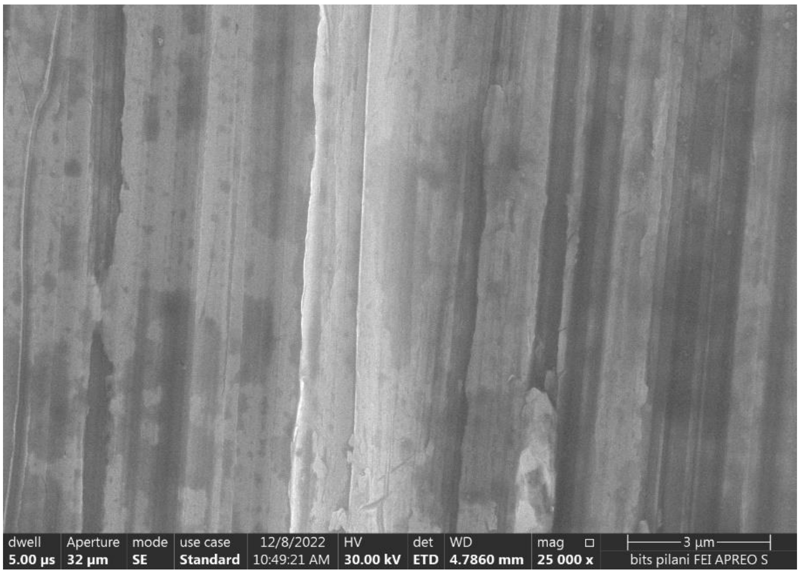

Figure 16- Poor polishing of the sample heated by microwaves for 30 minutes.

Chapter 5

Future Work

This study shows scope for abundant future work. Mechanical properties of microwave heated SLM-built Stainless Steel 316L can be found. Tensile tests, torsion tests, buckling tests, and fatigue tests can be performed. Knowing the properties of microwave heated SS316L manufactured by SLM or other AM technologies, the focus can shift to applications and component implementation.

In addition to SS316L, other materials should be studied in a similar way to observe whether or not microwaved affect them similarly. With the recent focus on additively manufactured magnetic materials, there is likely going to be a large surge for microwave processing of such materials.

Bibliography

[1] Oerlikon Additive Manufacturing Stainless Steel 316L

[2] ASTM International Standard Test Methods for Tension Testing of Metallic Materials

[3] Herzog, Dirk, Vanessa Seyda, Eric Wycisk, and Claus Emmelmann. "Additive manufacturing of metals." *Acta Materialia* 117 (2016): 371-392.

[4] Saeidi, Kamran, X. Gao, Yuan Zhong, and Zhijian James Shen. "Hardened austenite steel with columnar sub-grain structure formed by laser melting." *Materials Science and Engineering: A* 625 (2015): 221-229.

[5] Cruz, V., Q. Chao, N. Birbilis, D. Fabijanic, P. D. Hodgson, and S. Thomas. "Electrochemical studies on the effect of residual stress on the corrosion of 316L manufactured by selective laser melting." *Corrosion Science* 164 (2020): 108314.

[6] Smith, Thale R., Joshua D. Sugar, Chris San Marchi, and Julie M. Schoenung. "Strengthening mechanisms in directed energy deposited austenitic stainless steel." *Acta Materialia* 164 (2019): 728-740.

[7] Qiu, Chunlei, Mohammed Al Kindi, Aiman Salim Aladawi, and Issa Al Hatmi. "A comprehensive study on microstructure and tensile behaviour of a selectively laser melted stainless steel." *Scientific reports* 8, no. 1 (2018): 1-16.

[8] Zhang, Bi, Yongtao Li, and Qian Bai. "Defect formation mechanisms in selective laser melting: a review." *Chinese Journal of Mechanical Engineering* 30, no. 3 (2017): 515-527.

[9] Boban, Jibin, and Afzaal Ahmed. "Improving the surface integrity and mechanical properties of additive manufactured stainless steel components by wire electrical discharge polishing." *Journal of Materials Processing Technology* 291 (2021): 117013.

[10] Li, Jian, Jing Hu, Yi Zhu, Xiaowen Yu, Mengfei Yu, and Huayong Yang. "Surface roughness control of root analogue dental implants fabricated using selective laser melting." *Additive Manufacturing* 34 (2020): 101283.

[11] Jiang, Hua-Zhen, Zheng-Yang Li, Tao Feng, Peng-Yue Wu, Qi-Sheng Chen, Yun-Long Feng, Shi-Wen Li, Huan Gao, and He-Jian Xu. "Factor analysis of selective laser melting process parameters with normalised quantities and Taguchi method." *Optics & Laser Technology* 119 (2019): 105592.

[12] Gu, Dongdong, and Yifu Shen. "Balling phenomena in direct laser sintering of stainless steel powder: Metallurgical mechanisms and control methods." *Materials & Design* 30, no. 8 (2009): 2903-2910.

[13] Zhou, Chengshuang, Shiyin Hu, Qiaoying Shi, Huimin Tao, Yangyang Song, Jinyang Zheng, Peng Xu, and Lin Zhang. "Improvement of corrosion resistance of SS316L manufactured by selective laser melting through subcritical annealing." *Corrosion Science* 164 (2020): 108353.

[14] Benarji, K., Y. Ravi Kumar, A. N. Jinoop, C. P. Paul, and K. S. Bindra. "Effect of heat-treatment on the microstructure, mechanical properties and corrosion behaviour of SS 316 structures built by laser directed energy deposition based additive manufacturing." *Metals and Materials International* 27, no. 3 (2021): 488-499.

[15] Chen, Nan, Guoqiang Ma, Wanquan Zhu, Andrew Godfrey, Zhijian Shen, Guilin Wu, and Xiaoxu Huang. "Enhancement of an additive-manufactured austenitic stainless steel by post-manufacture heat-treatment." *Materials Science and Engineering: A* 759 (2019): 65-69.

[16] Ahsan, Md RU, A. N. M. Tanvir, Gi-Jeong Seo, Brian Bates, Wayne Hawkins, Chanho Lee, P. K. Liaw, Mark Noakes, Andrzej Nycz, and Duck Bong Kim. "Heat-treatment effects on a bimetallic additively-manufactured structure (BAMS) of the low-carbon steel and austenitic-stainless steel." *Additive Manufacturing* 32 (2020): 101036.

[17] Pokharel, Reeju, L. Balogh, D. W. Brown, B. Clausen, G. T. Gray III, V. Livescu, S. C. Vogel, and S. Takajo. "Signatures of the unique microstructure of additively manufactured steel observed via diffraction." *Scripta Materialia* 155 (2018): 16-20.

[18] Mishra, Radha Raman, and Apurbba Kumar Sharma. "Microwave–material interaction phenomena: heating mechanisms, challenges and opportunities in material processing." Composites Part A: Applied Science and Manufacturing 81 (2016): 78-97.

[19] El Khaled, D., N. Novas, J. A. Gazquez, and F. Manzano-Agugliaro. "Microwave dielectric heating: Applications on metals processing." Renewable and Sustainable Energy Reviews 82 (2018): 2880-2892.

[20] Y. Zhang, D. K. Agrawal, J. Cheng and T. Slawecki, "Microwave Power Absorption Mechanism of Metallic Powders," in IEEE Transactions on Microwave Theory and Techniques, vol. 66, no. 5, pp. 2107-2115, May 2018,

[21] Manoj Gupta, Eugene Wong, Microwaves and Metals, Willey publications, 2007

[22] Hossain, Umar, Shaaz Ghouse, Kenneth Nai, and Jonathan RT Jeffers. "Controlling and testing anisotropy in additively manufactured stochastic structures." *Additive Manufacturing* 39 (2021): 101849.

[23] Brytan, Z. "Comparison of vacuum sintered and selective laser melted steel AISI 316L." *Archives of Metallurgy and Materials* 62 (2017).

[24] Guo, Peng, Bin Zou, Chuanzhen Huang, and Huabing Gao. "Study on microstructure, mechanical properties and machinability of efficiently additive manufactured AISI 316L

stainless steel by high-power direct laser deposition." *Journal of Materials Processing Technology* 240 (2017): 12-22.

[25] Lei, Jianbo, Jichang Xie, Shengfeng Zhou, Heyu Song, Xinling Song, and Xiaoyu Zhou. "Comparative study on microstructure and corrosion performance of 316 stainless steel prepared by laser melting deposition with ring-shaped beam and Gaussian beam." *Optics & Laser Technology* 111 (2019): 271-283.

[26] Roy, R., Agrawal, D., Cheng, J. et al. Full sintering of powdered-metal bodies in a microwave field. Nature 399, 668–670 (1999)

[27] Mahmoudi, Mohamad, Alaa Elwany, Aref Yadollahi, Scott M. Thompson, Linkan Bian, and Nima Shamsaei. "Mechanical properties and microstructural characterization of selective laser melted 17-4 PH stainless steel." *Rapid Prototyping Journal* (2017).

[28] Saeidi, Kamran, X. Gao, Yuan Zhong, and Zhijian James Shen. "Hardened austenite steel with columnar sub-grain structure formed by laser melting." *Materials Science and Engineering: A* 625 (2015): 221-229.

[29] Mohd Yusuf, Shahir, Yifei Chen, Richard Boardman, Shoufeng Yang, and Nong Gao. "Investigation on porosity and microhardness of 316L stainless steel fabricated by selective laser melting." *Metals* 7, no. 2 (2017): 64.

[30] Tian, Qiwen. "The Development Status of Selective Laser Melting Technology (SLM)." In *Journal of Physics: Conference Series*, vol. 1798, no. 1, p. 012045. IOP Publishing, 2021.

[31] Majeed, Arfan, Altaf Ahmed, Abdus Salam, and Muhammad Zakir Sheikh. "Surface quality improvement by parameters analysis, optimization and heat treatment of AlSi10Mg parts manufactured by SLM additive manufacturing." *International Journal of Lightweight Materials and Manufacture* 2, no. 4 (2019): 288-295.

[32] "MICROWAVE APPLICATIONS." National Research Council. 1994. Microwave Processing of Materials. Washington, DC: The National Academies Press.

[33] Renaux, Maxence, Damien Méresse, Julien Pellé, Anthony Thuault, Céline Morin, Christelle Nivot, and Christian Courtois. "Mechanical modelling of microwave sintering and experimental validation on an alumina powder." Journal of the European Ceramic Society (2021).

[34] Tian, Qiwen. "The Development Status of Selective Laser Melting Technology (SLM)." In *Journal of Physics: Conference Series*, vol. 1798, no. 1, p. 012045. IOP Publishing, 2021.

[35] Gupta, Prateek, and Sudhir Kumar. "Investigation of stainless steel joint fabricated through microwave energy." *Materials and Manufacturing Processes* 29, no. 8 (2014): 910-915.